Journal of Physics: Conference Series **264** (2011) 012013 doi:10.1088/1742-6596/264/1/012013

Universal structure of a strongly interacting Fermi gas

Eva Kuhnle, Paul Dyke, Sascha Hoinka, Michael Mark, Hui Hu, Xia-Ji Liu, Peter Drummond, Peter Hannaford and Chris Vale

ARC Centre of Excellence for Quantum Atom Optics, Swinburne University of Technology, Hawthorn 3122, Australia

E-mail: cvale@swin.edu.au

Abstract. This paper presents studies of the universal properties of strongly interacting Fermi gases using Bragg spectroscopy. We focus on pair-correlations, their relationship to the contact $\mathcal{C}$ introduced by Tan, and their dependence on both the momentum and temperature. We show that short-range pair correlations obey a universal law, first derived by Tan through measurements of the static structure factor, which displays a universal scaling with the ratio of the contact to the momentum $\mathcal{C}/q$. Bragg spectroscopy of ultracold ^{6}Li atoms is employed to measure the structure factor for a wide range of momenta and interaction strengths, providing broad confirmation of this universal law. We show that calibrating our Bragg spectra using the f-sum rule leads to a dramatic improvement in the accuracy of the structure factor measurement. We also measure the temperature dependence of the contact in a unitary gas and compare our results to calculations based on a virial expansion.

1. Introduction

Universality is a striking feature of certain classes of interacting Fermi systems. When the range of the interparticle scattering potential r_0 is much smaller than the mean interparticle spacing $n^{-1/3}$ and the s-wave scattering length a, which characterises elastic collisions is large compared to $n^{-1/3}$, the system may display universal properties. Here, universality means that all dilute Fermi systems with sufficiently strong interactions behave identically on a scale given by the average particle separation, independent of the details of the short range interaction. Two component gases of fermionic atoms near a Feshbach resonance are an excellent system in which to achieve this universal regime in a precisely controlled manner [1–3]. With the discovery of universality in the Bose-Einstein condensate (BEC) to Bardeen-Cooper-Schrieffer (BCS) crossover, ultracold Fermi gases near Feshbach resonances have become a central topic in atomic physics [4–10].

Understanding these strongly interacting Fermi gases, however, can present significant challenges for theorists [11]. As the scattering length becomes large it can no longer be treated as a small parameter and perturbative theories, which have had wide success for weakly interacting Bose gases, cannot be applied. In 2005 Shina Tan made dramatic progress by deriving several exact relations valid through the BEC-BCS crossover, which relate the microscopic properties of the constituent particles to bulk thermodynamic quantities [12–14]. These exact relations are applicable in broad circumstances: zero or finite temperatures, superfluid or normal phases,

homogeneous or trapped systems, and in few or many-body systems. Tan invoked a new quantity in his theory, called the contact $\mathcal{C}$. The contact is defined as

$$\mathcal{C} = \lim_{k\to\infty} n_k k^4 \tag{1}$$

where n_k is the momentum density as a function of the wavevector k. At large k, this density profile has a $1/k^4$ dependence so the contact is a constant which depends on the strength of the two-body interactions. A more physically intuitive picture of the contact was also given by Tan as the number of closely spaced spin-up/spin-down pairs, i.e., $\mathcal{C}$ quantifies the likelihood of finding two fermions with opposite spin close enough to interact with each other. In systems with a large scattering length where the range of the interaction potential r_0 is negligible, this single parameter encapsulates all of the information required to determine the many-body properties [15, 16]. $\mathcal{C}$ depends upon two quantities, the dimensionless interaction parameter $1/(k_F a)$, where k_F is the Fermi wavevector and the relative temperature of the system T/T_F, where T_F is the Fermi energy divided by Boltzmann's constant. The contact $\mathcal{C}$ was first extracted [17] from the number of closed-channel molecules determined through photo-association [8] and Tan's adiabatic and virial relations were very recently verified experimentally [18]. Both of these studies investigated the interaction dependence of the $\mathcal{C}$. We will generally refer to the dimensionless contact $\mathcal{I}$ given by $\mathcal{C}/(Nk_F)$, where N is the number of particles.

2. Structure factor in the unitary limit - a universal quantity

Tan's exact analytic relations link various many-body quantities such as the total energy and momentum distribution to the short-range parameter $\mathcal{I}$. Short-range structure in a quantum fluid depends upon the relative wave-function of the interacting particles, in this case fermions in different spin states. In a two-component (spin-up/spin-down) Fermi gas this is given by $\psi_{\uparrow\downarrow}(r) \propto 1/r - 1/a$, where a is the s-wave scattering length. Tan used this to show that, for length scales $r_0 < r < 1/k_F$, the spin-antiparallel pair correlation function is given exactly by Eq. (2) which includes the contact as a pre-factor [12]

$$g^{(2)}_{\uparrow\downarrow}(r) = \frac{\mathcal{C}}{16\pi^2}\left(\frac{1}{r^2} - \frac{2}{ar}\right). \tag{2}$$

Such pair correlation functions are difficult to measure directly in ultracold gases; however, it is possible to measure macroscopic quantities which depend on correlation functions in a well defined way. A prime example is the static structure factor, $S(k)$, which is given by the Fourier transform of $g^{(2)}(r)$ ($q = \hbar k$ is the probe momentum). In a two component Fermi gas with an equal number of particles in each state N, the structure factor consists of two components, corresponding to correlations between particles in the same state and particles in different states $S(k) = S_{\uparrow\uparrow}(k) + S_{\uparrow\downarrow}(k)$. When the momentum is much larger than the Fermi momentum, particles in the same state will be uncorrelated and $S_{\uparrow\uparrow}(k \gg k_F) \simeq 1$, so all variation in $S(k)$ will then be due to changes in $S_{\uparrow\downarrow}(k)$ [19, 20]. The Fourier transform of Eq. (2) yields the following for $S_{\uparrow\downarrow}(k)$

$$S_{\uparrow\downarrow}(k \gg k_F) = \frac{\mathcal{I}}{4}\frac{k_F}{k}\left[1 - \frac{4}{\pi k_F a}\left(\frac{k_F}{k}\right)\right], \tag{3}$$

which has a straightforward dependence upon $\mathcal{I}$, the relative probe momentum k/k_F, and the interaction strength $1/(k_F a)$. At unitarity, $a \to \infty$, the second term vanishes and $S(k)$ varies linearly with k_F/k. Rewriting Tan's relation in this way points to a method to experimentally verify Tan's universal relation for pair correlations between spin-up/spin-down fermions since the static structure factor can readily be measured using Bragg spectroscopy.

3. Verification of Tan's universal pairing law

Inelastic scattering experiments are a well established technique to probe both the dynamic and static structure factors of many-body quantum systems [21]. Ultracold atoms are highly amenable to inelastic scattering through Bragg spectroscopy which has previously been used to measure both the dynamic [22, 23] and static structure factors [24, 25] of atomic Bose-Einstein condensates. In ultracold Fermi gases Bragg spectroscopy was used to measure both the dynamic and static structure factors over the BEC-BCS crossover, albeit at a single momentum [20]. The ability to vary the momentum differentiates Bragg spectroscopy from rf spectroscopy [26, 27], providing access to a broad range of the excitation spectrum and avoiding final state interaction effects as no third atomic state is involved.

Conceptually, one can understand how Bragg spectroscopy probes the contact (the number of closely spaced spin-up/spin-down pairs). The spatial period of the Bragg lattice ($\lambda_{Br} = k^{-1}$) sets the size scale being probed. Pairs, whose size is small compared to λ_{Br} can be scattered as single particles with twice the atomic mass ($2m$). Varying the ratio k/k_F we can map the fraction of pairs within a particular size range $0 < r < \lambda_{Br}$. At unitarity, these short-range pair correlations grow linearly with λ_{Br}, Eq. (3).

To demonstrate the validity of Eq. (3) we perform measurements of $S(k)$ for a range of momenta (k/k_F) and at different values of the interaction parameter $1/(k_F a)$. We start by preparing clouds containing $N \approx 3 \times 10^5$ ^{6}Li atoms in an equal mixture of the two lowest lying ground states $|F = 1/2, m_F = \pm 1/2\rangle$ evaporatively cooled in a single beam optical dipole trap ($\lambda = 1075$ nm) at a magnetic field of 834 G [31]. Next, we adiabatically ramp up a second far detuned laser ($\lambda = 1064$ nm) which intersects the first trapping beam at an angle of 74° forming a crossed beam dipole trap. By appropriately selecting the intensities of each of the two trap lasers we tune the mean harmonic confinement frequency of the crossed trap $\bar{\omega}$ over the range $\bar{\omega} = 2\pi \times (38 - 252)$ s^{-1} while the aspect ratio, $\omega_{x,y}/\omega_z$, varies from 3.4 to 16. Controlling the trap frequencies in this way allows us to tune the atom density and hence the Fermi wavevector over a broad range. Once in the final crossed beam trap, we ramp the magnetic field to select the scattering length a which gives the desired value of $1/(k_F a)$. This allows us to tune k_F and $1/(k_F a)$ independently. The cloud is then held at the final magnetic field for a time $\tau \gg 10\,\bar{\omega}^{-1}$ to reach equilibrium before applying the Bragg pulse and imaging at that magnetic field.

Bragg scattering is achieved by illuminating these ^{6}Li clouds with two counter propagating laser beams with a small frequency difference δ. This creates a standing wave which moves with velocity δ/k_{Br} where $k_{Br} = 2\pi/\lambda_{Br}$ and $\lambda_{Br} = 671\,\text{nm}$ is the wavelength of the light used for Bragg scattering. Resonant Bragg scattering occurs when the energy difference between the two beams is equal to the energy required to eject a particle from the cloud with momentum $2\hbar k_{Br}$. The lasers used for Bragg scattering are approximately 2 GHz red-detuned from the two ground hyperfine states which is large compared to the ~ 80 MHz splitting between the $|1/2, \pm 1/2\rangle$ states. This means that both states are coupled approximately equally to the Bragg beams (to within 4%).

To measure the static structure factor $S(k)$ we begin by recording a Bragg spectrum. This consists of measuring the momentum transferred to the cloud by the Bragg lasers as a function of δ. The transferred momentum is directly proportional to the resultant centre of mass displacement $\Delta X(k, \delta)$ measured after 2 ms time of flight [20]. A Bragg spectrum for a unitary gas is shown in the inset of Fig. 1 for $k/k_F = 8.5$ as a function of the Bragg frequency δ. At this momentum, the pair and free-atom excitations are clearly distinguished at frequencies of ~ 150 kHz and ~ 300 kHz, respectively. The Bragg pulse duration, 50 μs, is short compared to the two-photon Rabi cycling period, ensuring that spectra are obtained in the linear response regime.

The centre of mass displacement, $\Delta X(k, \delta)$, is proportional to the convolution of the spectral content of the Bragg pulse and the dynamic structure factor of the gas $S(k, \delta)$ [28]. The

proportionality constant depends upon the two-photon Rabi frequency Ω_{Br} which can be difficult to measure accurately. Integrating $\Delta X(q,\delta)$ over δ yields a number proportional to the static structure factor, $S(k) = \hbar N^{-1} \int S(k,\delta) d\delta$, but Ω_{Br} remains unknown. We overcome the need to find Ω_{Br} by invoking the f-sum rule [21]: $NE_r = \int S(k,\delta)\delta d\delta$, where $E_r = 2\hbar^2 k_{Br}^2/m$ is the two-photon recoil energy. As both $S(k)$ and the f-sum rule involve N, we normalise the area under each measured spectra using

$$S(k) = \frac{2\hbar k_{Br}^2}{m} \frac{\int \Delta X(k,\delta) d\delta}{\int \Delta X(k,\delta)\delta d\delta}, \tag{4}$$

where the constant involving Ω_{Br} appears before each integral and therefore cancels. Equation (3) is absolute, requiring only knowledge of the recoil energy, which can be determined with high accuracy, leading to an accurate measure of $S(k)$.

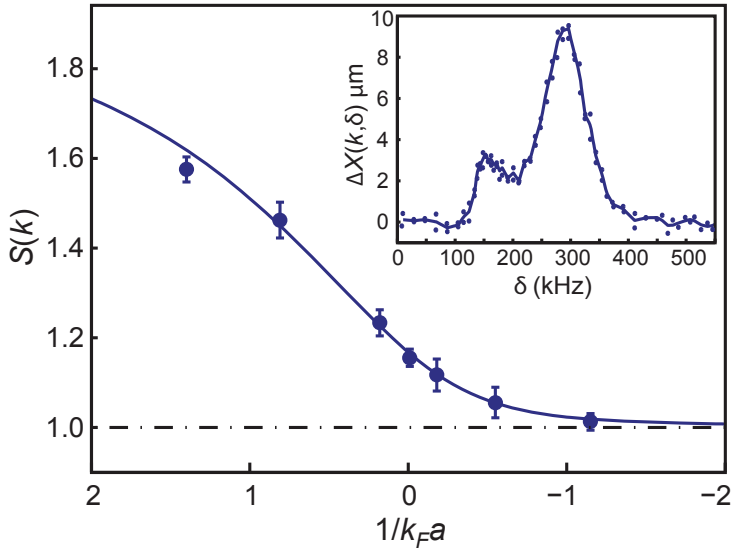

Figure 1. Static structure factor in the BEC-BCS crossover. Experimental points were obtained by integrating Bragg spectra normalized via the f-sum rule for $k/k_F = 4.8$. Error bars are due to shot to shot atom number fluctuations and uncertainties in measuring centre of mass. The theoretical line is a zero temperature result, calculated by interpolating the near-resonance structure factor Eq. (2) with the asymptotic results in the BCS and BEC limits. Inset: A Bragg spectrum obtained at $1/(k_F a) = 0$ and $k/k_F = 8.5$ showing centre of mass displacement $\Delta X(k,\delta)$ versus Bragg frequency δ. Points are single shots and the line is a guide to the eye. The pair ($\delta \sim 150$ kHz) and free atom peaks ($\delta \sim 300$ kHz) are clearly distinguished.

3.1. Interaction dependence

Bragg spectra reflect the composition of the gas, being dominated by bosonic molecules below the Feshbach resonance, pairs and free fermionic atoms near unitarity, and free fermions above resonance. To reveal the effects of interactions, scattering of trapped gases has to be considered [20]. This can be complicated by elastic collisions between scattered and unscattered particles which are hard to separate in the BEC-BCS crossover. Here, elastic collisions help as they preserve centre of mass motion, so $\Delta X(k,\delta)$ is a good measure of the Bragg signal throughout the BEC-BCS crossover, independent of cloud shape and scattering length. We have previously

measured Bragg spectra across the BEC-BCS crossover at a momentum of $k/k_F = 4.8$ and observed a smooth transition in $S(k, \delta)$ from being dominated by molecular excitations below the Feshbach resonance to atomic excitations above resonance. From such spectra, we can obtain $S(k)$ using Eq. 4 as plotted in Fig. 1 which shows excellent agreement with the zero temperature theoretical calculation. This shows that we can quantitatively measure pair correlations at a given momentum using Bragg spectroscopy.

3.2. Momentum dependence

Next we come to the measurement of $S(k)$ as a function of k/k_F [29]. At unitarity we expect $S(k)$ to vary linearly with k_F/k according to Eq. (2). Rather than changing k directly by varying the angle between the two Bragg beams, we change $k_F = (48N)^{1/6}\sqrt{m\bar{\omega}/\hbar}$ by varying $\bar{\omega} = (\omega_x\omega_y\omega_z)^{1/3}$, the geometric mean frequency of the optical dipole trap. Universality allows us to change the relative length scale being probed simply by changing the density of the gas. Using the crossed beam optical trap described above we can tune $\bar{\omega}$ such that the Fermi wavevector can be tuned anywhere over the range $k_F = 2.1\ \mu\text{m}^{-1}$ - $5.3\ \mu\text{m}^{-1}$, or $k/k_F = 3.5$-9.1. A sequence of Bragg spectra were obtained for gases at three values of $1/(k_Fa) = +0.3$, 0.0 and -0.2, while varying k_F. From these, $S(k)$ was extracted and the results are plotted in Fig. 2. The solid lines are the prediction from Eq. (2) using the zero temperature contact with no free parameters. The experimental points closely follow the theory, confirming the exact analytic dependence of $S_{\uparrow\downarrow}(k) \cong S(k) - 1$ on q, Eq. (2). At unitarity $1/(k_Fa) = 0$, the dependence on a vanishes and a straight line fit (dashed line) shows the simple universal behavior of fermionic pairing. The fitted slope of 0.75 ± 0.03 is slightly below the zero temperature prediction of 0.81 which may be due to reduced pairing at the finite temperature ($T/T_F = 0.10 \pm 0.02$ at unitarity) discussed in the next section. This result is in good agreement with the contact evaluated from the equation of state of a homogeneous gas measured by the ENS group [10]. At $1/(k_Fa) = +0.3$ the data depart from a straight line displaying the downward curvature consistent with the first order term in Eq. (2). A similar upward curvature is seen at $1/(k_Fa) = $ -0.2. Our simple relation Eq. (2) is seen to accurately describe $S(k)$ on both sides of the Feshbach resonance demonstrating the wide applicability of the Tan relations.

4. Temperature dependence of $\mathcal{I}$

As discussed in section 1, the contact $\mathcal{I}$ depends on both the interaction parameter and the relative temperature. Here we look at the latter dependence in a unitary Fermi gas where the spin-up/spin-down static structure factor is given by $S_{\uparrow\downarrow}(k) = \frac{\mathcal{I}}{4}\frac{k_F}{k}$. Any variation in the measured structure factor with temperature is then linearly related to the contact. For this series of measurements we use a lower relative momentum of $k/k_F = 2.7$ to enhance the contribution of $S_{\uparrow\downarrow}(k)$ to $S(k)$. This was achieved by reducing the angle between the two Bragg beams to 49° which reduces the atomic recoil frequency to 51 kHz. The lower momentum also means that all Bragg scattered atoms now remain trapped after the Bragg pulse as the energy imparted to the atoms/pairs by the Bragg pulse is lower than the trap depth. This makes possible a second means of determining $S(k)$ from measurements of the increase in the mean square cloud width to determine the energy imparted by the Bragg pulse. The details of this measurement scheme will be published elsewhere [30], but here we note that this method provides an alternative means to determine $S(k)$ that we can compare to our measurements of the momentum imparted by the Bragg pulse through centre of mass displacement. Figure 3 shows the measured structure factors (left axis) and the corresponding contact (right axis) measured as a function of temperature. The different temperatures were obtained by evaporating down to the lowest temperature and then releasing and recapturing atoms in the optical trap and holding for 800 ms to allow rethermalisation. In this way we could repeatably vary the temperature over the range $0.1 \rightarrow 1T_F$ while holding N and the trapping parameters

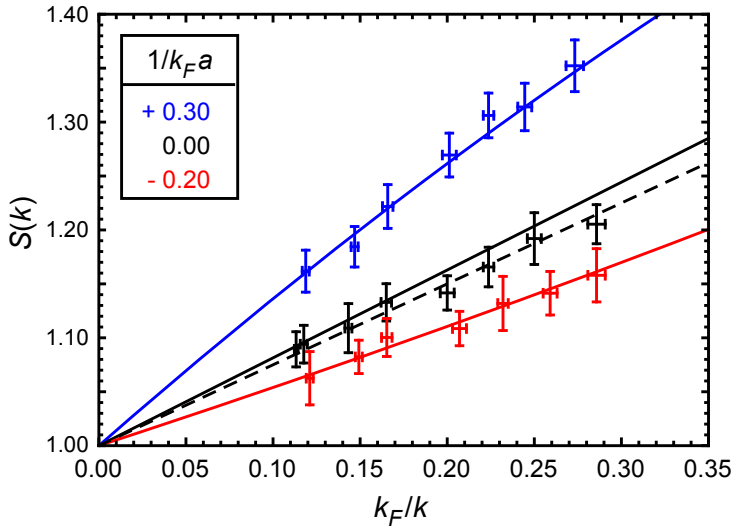

Figure 2. Universal dependence of the static structure factor of a strongly interacting Fermi superfluid. Measured and calculated static structure factor versus k_F/k for $1/(k_F a) = +0.3$, 0.0, and -0.2. Bragg momentum k is fixed while k_F is varied by changing the mean trapping frequency $\bar{\omega}$. Vertical error bars are due to atom number fluctuations and uncertainties in measuring the centre of mass and horizontal error bars are due to atom number fluctuations and uncertainties in $\bar{\omega}$. Solid lines are the zero temperature theory and the dashed line is a straight line fit to the $1/(k_F a) = 0$ data yielding a slope of 0.75 ± 0.03.

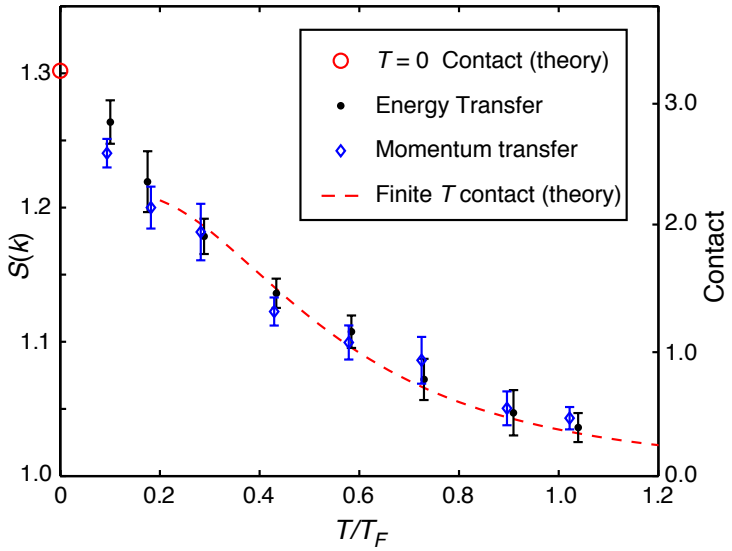

Figure 3. Temperature dependence of the static structure factor and contact for unitary Fermi gas. Open circles are the structure factors measured using centre of mass displacement as in section 3 and filled circles are the structure factors measured via the energy transferred to the cloud. The large open circle represents the zero temperature calculated contact and the dashed red line is a theoretical calculation based on the quantum virial expansion [32].

constant, by varying the time between release and recapture. Also shown in the figure are the calculated zero temperature contact $\mathcal{I} = 3.26$ (large red open circle) and finite temperature contact determined via a virial expansion calculation (red dashed line) [32]. The contact decays monotonically with increasing temperature reflecting the decay of pair correlations and agrees well with the theoretical prediction. We note that the critical temperature for superfluidity occurs around $0.2\,T_F$ and, while the data points near the critical temperature are relatively sparse, we do not observe any striking features near this point. It is also clear that pair correlations at this momentum persist well above the critical temperature, up to nearly the Fermi temperature. While this measurement only quantifies pair correlations at a particular momentum it does indicate that the build up of such correlations is relatively gradual and begins at high temperature.

5. Conclusions

In summary, we have shown that the structure factor of a strongly interacting ultracold Fermi gas follows a universal law which is a direct consequence of Tan's relation for the pair correlation functions. Our measurements provide one of the first demonstrations of a broadly applicable exact result for Fermi gases in the BEC-BCS crossover. We also provide the first measurements of the temperature dependence of the contact in a unitary Fermi gas and find good agreement with theoretical calculations based on the virial expansion. Bragg spectroscopic measurements provide a useful means to quantify pairing and to quantitatively map the phase diagram of the BEC-BCS crossover. In future work we will utilise low momentum Bragg spectroscopy to probe pairing at momenta nearer the Fermi momentum which may offer insight into pseudogap pairing.

This work is supported by the Australian Research Council Centre of Excellence for Quantum-Atom Optics and Discovery Projects DP0984522 and DP0984637.

6. References

[1] Heiselberg H 2001 *Phys. Rev. A* **63** 043606
[2] Ho T-L 2004 *Phys. Rev. Lett.* **92** 090402
[3] Hu H, Drummond P D and Liu X-J 2007 *Nat. Phys.* **3** 469
[4] Jochim S, Bartenstein M, Altmeyer A, Hendl G, Riedl S, Chin C, Hecker-Denschlag J and Grimm R 2003 *Science* **302** 2101
[5] Greiner M, Regal C A and Jin D S 2003 *Nature* **426** 537
[6] Zwierlein M W, Abo-Shaeer J R, Schirotzek A, Schunck C H and Ketterle W 2005 *Nature* **435** 1047
[7] Kinast J, Turlapov A, Thomas J E, Chen Q, Stajic J and Levin K 2005 *Science* **307** 1296
[8] Partridge G B, Strecker K E, Kamar R I, Jack M W and Hulet R G 2005 *Phys. Rev. Lett.* **95** 020404
[9] Nascimbene S, Navon N, Jiang K J, Chevy F and C. Salomon 2010 *Nature* **463** 1067 (2010)
[10] Navon N, Nascimbene S, Chevy F and Salomon C 2010 *Science* **328** 729
[11] Giorgini A, Pitaevskii L P and Stringari A 2008 *Rev. Mod. Phys.* **80** 1215
[12] S. Tan 2008 *Ann. Phys.* **323** 2952
[13] S. Tan 2008 *Ann. Phys.* **323** 2971
[14] S. Tan 2008 *Ann. Phys.* **323** 2987
[15] Braaten E and Platter L 2008 *Phys. Rev. Lett.* **100** 205301
[16] Zhang S and Leggett A J 2009 *Phys. Rev. A* **79** 023601
[17] Werner F, Tarruell L and Castin Y 2009 *Eur. Phys. J. B* **68** 401
[18] Stewart J T, Gaebler J P, Drake T E and Jin D S 2010 *Phys. Rev. Lett.* **104** 235301
[19] Combescot R, Giorgini S and Stringari S 2006 *Europhys. Lett.* **75** 695
[20] Veeravalli G, Kuhnle E, Dyke P and Vale C J 2008 *Phys. Rev. Lett.* **101** 250403
[21] Pines D and Nozières P 1966 *The Theory of Quantum Liquids, Vol. I* (Benjamin, New York)
[22] Stenger J, Inouye S, Chikkatur A P, Stamper-Kurn D M, Pritchard D E and Ketterle W 1999 *Phys. Rev. Lett.* **82** 4569
[23] Zambelli F, Pitaevskii L P, Stamper-Kurn D M and Stringari S 2000 *Phys. Rev. A* **61** 063608
[24] Stamper-Kurn D M, Chikkatur A P, Grlitz A, Inouye S, Gupta S, Pritchard D E and Ketterle E 1999 *Phys. Rev. Lett.* **83** 2876

[25] Steinhauer J, Ozeri R, Katz N and Davidson N 2002 *Phys. Rev. Lett.* **88** 120407
[26] Schunck C H, Shin Y, Schirotzek A and Ketterle W 2008 *Nature* **454** 739
[27] Stewart J T, Gaebler J P and Jin D S 2008 *Nature* **454** 744
[28] Brunello A, Dalfovo F, Pitaevskii L, Stringari S and Zambelli F 2001 *Phys. Rev. A* **64** 063614
[29] Kuhnle E, Hu H, Liu X-J, Dyke P, Mark M, Drummond P D, Hannaford P and Vale C J 2010 *Phys. Rev. Lett.* **105** 070402
[30] Kuhnle E, Hu H, Dyke P, Hoinka S, Hannaford P and Vale C J 2010 in preparation
[31] Fuchs J, Duffy G J, Veeravalli G, Dyke P, Bartenstein M, Vale C J, Hannaford P and Rowlands W J 2007 *J. Phys. B: At. Mol. Opt. Phys.* **40** 4109
[32] Liu X-J, Hu H and Drummond P D 2009 *Phys. Rev. Lett.* **102** 160401